Conformational Preferences of Ethyl Propionate Molecule: Raman, Temperature Dependent FTIR Spectroscopic Study Aided by ab Initio Quantum Chemical and Car–Parrinello Molecular Dyna...

ARTICLE *in* THE JOURNAL OF PHYSICAL CHEMISTRY A · MAY 2013

Impact Factor: 2.69 · DOI: 10.1021/jp404247v · Source: PubMed

4 AUTHORS, INCLUDING:

Bipan Dutta
Sammilani Mahavidyalaya
15 PUBLICATIONS **9** CITATIONS
SEE PROFILE

Joydeep Chowdhury
Jadavpur University
71 PUBLICATIONS **631** CITATIONS
SEE PROFILE

THE JOURNAL OF PHYSICAL CHEMISTRY A

Article

pubs.acs.org/JPCA

Conformational Preferences of Ethyl Propionate Molecule: Raman, Temperature Dependent FTIR Spectroscopic Study Aided by ab Initio Quantum Chemical and Car−Parrinello Molecular Dynamics Simulation Studies

Bipan Dutta,[†] Takeyuki Tanaka,[‡] Arup Banerjee,[§] and Joydeep Chowdhury*[,†]

[†]Department of Physics, Sammilani Mahavidyalaya, E.M. Bypass, Baghajatin Station, Kolkata 700 075, India

[‡]Integrated Center for Sciences, Ehime University, 3-5-7 Tarumi, Matsuyama, Ehime 790-8566, Japan

[§]Department of Spectroscopy, Indian Association for the Cultivation of Science, Jadavpur, Kolkata 700 032, India

Supporting Information

ABSTRACT: The conformational preferences of the industrially significant ethyl propionate (EP) molecule have been investigated from the Raman and FTIR spectra, aided by ab initio and Car−Parrinello molecular dynamics (CPMD) simulation studies. The vibrational signatures of various rotameric forms of the EP molecule have been assigned for the first time from the potential energy distributions (PEDs). The critical analyses of the vibrational signatures reveal the coexistences of the Trans−Trans (TT), Trans−Antigauche (TG^-) [Trans−Gauche (TG^+)], Antigauche−Trans (G^-T) [Gauche−Trans (G^+T)], Antigauche−Antigauche (G^-G^-) [Gauche−Gauche (G^+G^+)], and Gauche−Antigauche (G^+G^-) [Antigauche−Gauche (G^-G^+)] forms of the EP molecule at room and at high temperatures. However, at low temperature (ca. 70 °C), the TT and TG^- forms of the EP molecule is estimated to be preponderant. The Car−Parrinello molecular dynamics simulation studies of the EP molecule estimated at high, room, and low temperatures are also in harmony with our conjecture as suggested from the vibrational analyses. The ab intio molecular dynamics simulations are observed to be a useful tool for the conformational analyses of the molecule.

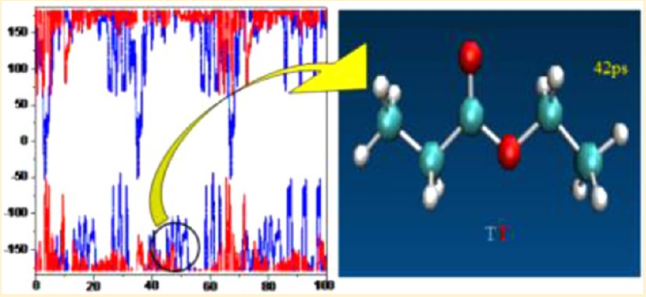

1. INTRODUCTION

Ethyl propionate (EP) is the ethyl ester of propionic acid. It has a pineapple like odor,[1] and fruits like kiwis and strawberries naturally contain EP molecules.[2] Moreover, the EP molecule is the alkyl esters of ethyl alcohol, and it finds wide applications as biodiesel.[3] The importance concerning the production and the use of biodiesel have been stressed during the past decade due to concerns about environmental pollution, the possibility of future dearth of petroleum oil, and also looking for renewable energy sources. Considering the potent industrial applications of the EP molecule, here we report a detailed study on the IR spectra of the molecule recorded at high, room, and low temperatures. The Raman spectrum of the molecule in the liquid state at room temperature is also reported herewith. This paper may also be considered as the first report concerning the detailed vibrational analysis of the EP molecule aided by ab initio calculations. Interestingly, the EP molecule can exist in various rotameric forms ca. Trans−Trans (TT), Trans−Antigauche (TG^-) [enantiomeric form Trans−Gauche (TG^+)], Antigauche−Trans (G^-T) [enantiomeric form Gauche−Trans (G^+T)], Antigauche−Antigauche (G^-G^-) [enantiomeric form Gauche−Gauche (G^+G^+)], and Gauche−Antigauche (G^+G^-) [enantiomeric form Antigauche−Gauche (G^-G^+)] forms depending upon the rotation about C_1-C_2 and O_5-C_6 bonds. The possible existences of various forms of the EP molecule at high, room, and low temperatures have also been estimated from the vibrational signatures and also from the Car−Parrinello molecular dynamics (CPMD) simulation studies.

2. INSTRUMENTATION

The Raman spectrum of the EP molecule was obtained with a Renishaw Raman Microscope, equipped with a He−Ne laser excitation source emitting at a wavelength of 632.8 nm, and a Peltier cooled (−70 °C) charge coupled device (CCD) camera. A Leica microscope was attached and was fitted with three objectives (5×, 20×, and 50×). For these experiments, the 20× objective was used to focus the laser beam onto a spot of 1−2 μm^2. Laser power at the sample was 20 mW, and the data acquisition time was 30 s. The holographic grating (1800 grooves/mm) and the slit enabled the spectral resolution of 1 cm^{-1}. The mid-infrared spectra from 400 to 3500 cm^{-1} of the

Received: January 30, 2013
Revised: May 27, 2013
Published: May 28, 2013

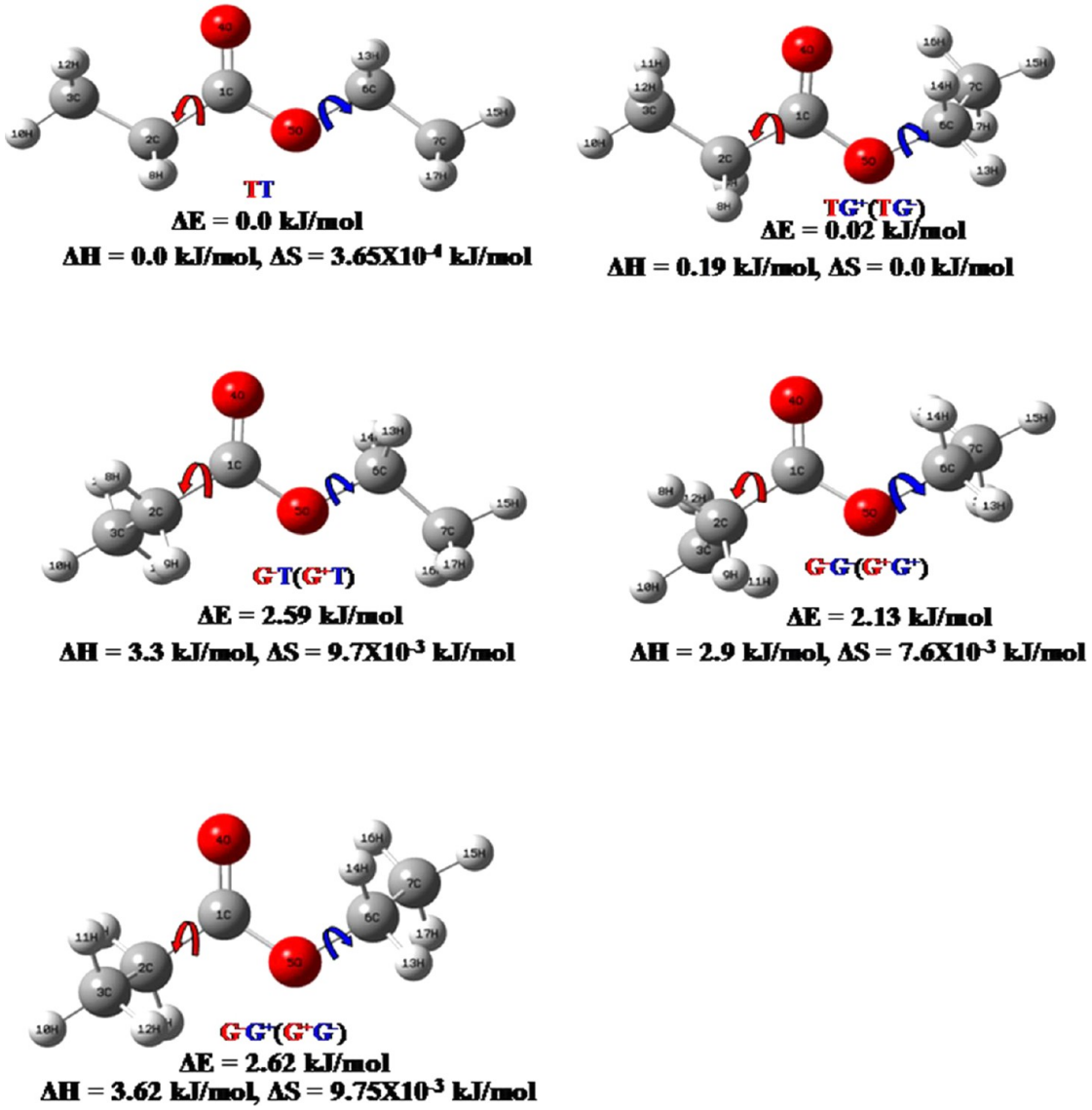

Figure 1. The optimized molecular structures and respective SCF energies of the various rotameric forms of the EP molecule as obtained from the MP2/aug-cc-PVTZ level of theory.

liquid EP molecule were recorded on a Perkin-Elmer model Spectrum 100 Fourier transform spectrometer equipped with a nichrome wire source, Ge/CsI beamsplitter, and DTGS detector. The spectrum of the liquid was obtained with the samples contained in 12 μm cells equipped with KBr windows. Atmospheric water vapor was removed from the spectrometer chamber by purging with dry nitrogen. The interferograms were recorded at variable temperatures ranging from 55 °C to −70 °C with 4 scans and transformed by a Blackman-Harris apodization function with a theoretical resolution of 1.0 cm^{-1}. The temperature studies were carried out in a specially designed cryostat cell, which is composed of a copper cell with a 4 μm path length and wedged silicon windows sealed to the cell with indium gaskets. The temperature was monitored by two platinum thermal resistors, and the cell was cooled by the vapors from boiling liquid nitrogen. The Fourier transform infrared (FTIR) spectrum of the annealed sample was achieved by heating the cell in vacuum until the temperature was reached at 55 °C. When the desired temperature was achieved, the cell was allowed to cool down to room temperature, and the spectrum was recorded.

3. THEORETICAL CALCULATIONS

The theoretical calculations were carried out using the Gaussion-09 program[4] operated in a linux system. Optimizations of the TT, TG^-, G^-T, G^-G^-, and G^+G^- rotameric forms of the EP molecule and vibrational frequencies at their respective optimized geometries were computed by the second-order Møller-Plesset (MP2)[5] levels of theory. However, the theoretically estimated vibrational frequencies, as obtained from the MP2/aug-cc-pVTZ level of theory, were scaled by the scaling factor 0.945. In the process of geometry optimization for the fully relaxed method using very tight criterion, convergence of all the calculations and absence of imaginary values in the wavenumbers confirmed the attainment of local minima on the potential energy surface. The normal coordinate analyses of the EP molecules were carried out based on Wison's GF Matrix method[6] by extracting the Cartesian force constant from the ab initio MP2 calculations. The local symmetry

dx.doi.org/10.1021/jp404247v | J. Phys. Chem. A 2013, 117, 4838−4850

coordinates were defined in the same way as reported elsewhere.[6b]

Ab initio molecular dynamics (MD) simulations have been carried out using the CPMD program[7] with the preoptimized TT rotameric form of the EP molecule. In the CPMD approach, the explicit time scale separation of the fast moving electrons with respect to the slow nuclear motion, as suggested in the Born−Oppenheimer (BO) approximation, is exploited. The hybrid quantum/classical problems are mapped by considering the electronic structures of the EP molecule at successively frozen nuclear frames leading to a two component purely classical problem. The TT form of the EP molecule is placed in a simple cubic box of dimension 10.0 Å. The ab initio MD simulations were then executed in the NVT ensemble at various temperatures (ca. 25 °C, 55 °C, and −70 °C). The length of the CPMD trajectory was set at 100 ps with a time step of 4 au. The temperature of the ensemble was controlled through coupling to a Nose-Hoover thermostat.[8] An electronic fictitious mass parameter of 400 au has been employed in the simulation run. Electronic exchange and correlation have been modeled using gradient corrected Perdew, Burke, and Ernzerhof (PBE) functional.[9] Core electrons were treated using the norm-conserving atomic pseudopotentials (PP) of Ttoullier and Martins,[10] while valence electrons were represented in a plane-wave basis set truncated at an extended energy cutoff of 50 Ry. The simulated data and the respective snap shots were visualized using the VMD[11] visualization software.

4. RESULTS AND DISCUSSION

4.1. Molecular Structure. The EP molecule can exist in various rotameric forms (i.e., cis, trans, and gauche/antigauche). The self-consistent field (SCF) energy of the cis form of the EP molecule is ∼49 kJ/mol more than that of the corresponding trans and gauche/antigauche forms. The higher energy for the cis structure of the EP molecule may be attributed to steric hindrance and also may be due to intramolecular O···H hydrogen bond interaction. The molecular structures of the various rotameric trans, gauche/antigauche forms of the EP molecule are shown in Figure 1. The relative changes in the SCF energies, enthalpies, and entropies of the different forms of the EP molecule are also shown in Figure 1. The TG^+ (TG^-) is nearly of equal energy with that of the TT form of the EP molecule. The SCF energies of the $G^-T(G^+T)$, $G^-G^-(G^+G^+)$, and $G^-G^+(G^+G\_)$ forms of the molecule are ∼2−2.6 kJ/mol higher than the corresponding TT form of the EP molecule. However, due to the TG^+ and TG^- possibilities, the TG form is statistically more probable than the TT form of the EP molecule.

The selected optimized structural parameters, dipole moments, and rotational constants of the various TT, TG^-, G^-T, G^-G^-, and G^-G^+ forms of the EP molecule are shown in Table TS1. The C_1-C_2 bond length and the skeletal $C_1-C_2-C_3$ bond angle for the TT/TG^- form of a molecule are quite similar (1.51/1.50 Å and 112.33/112.39°), whereas for other forms of the molecule (i.e., $G^-T/G^-G^-/G^+G^-$), the bond angles in particular are considerably decreased (109.66/109.45/109.63°). Moreover the $O_5-C_6-C_7$ bond angle for the $TG^-/G^-G^-/G^+G^-$ forms of the molecule is significantly increased by ∼3.8° compared to the TT/G^-T form of the molecule. The theoretical results further indicate that both the carbon C_2 and C_6 atoms of the $-CH_3$ group of the TT, TG^-, G^-T, G^-G^-, and G^+G^- forms of the EP molecule are ∼sp^3 hybridized with the relevant bond angles ∼107.55° and 108.54°, respectively.

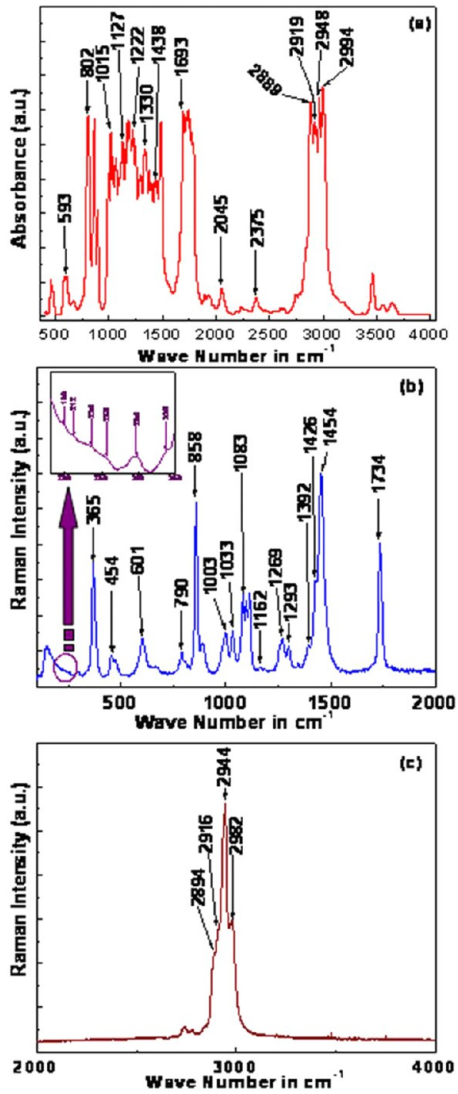

Figure 2. (a) The FTIR spectrum of the EP molecule in liquid state recorded at room temeperaure (25 °C). The Raman spectra of the EP molecule in the liquid state recorded at (b) 200−2000 cm^{-1} and (c) 2000−4000 cm^{-1} regions for λ_{exc} = 632.8 nm.

4.2. Raman, FTIR Spectrum of the EP Molecule, and Their Vibrational Assignment. The five rotameric forms of the EP molecule, as shown in Figure 1, have 17 atoms; hence, each of them has 45 fundamental vibrations. The four different forms (ca. TG^-, G^-T, G^-G^-, and G^+G^-) of the EP molecule belong to the C_1 point group symmetry, while the TT form belongs to C_s point group. The 45 fundamental vibrations of the TT form of the EP molecule with C_s point group symmetry are distributed among A' and A'' symmetry species as

$$\Gamma_{vib} = 27A' + 18A'' \quad (1)$$

Simple group theory predicts that 27 planar (A') and 18 nonplanar (A'') species are expected to appear both in Raman and in the FTIR spectra. However, among the vibrations originating from the TT form and the other rotameric TG^-, G^-T, G^-G^-, and G^+G^- forms of the EP molecule, some vibrations may be degenerate.

dx.doi.org/10.1021/jp404247v | J. Phys. Chem. A 2013, 117, 4838−4850

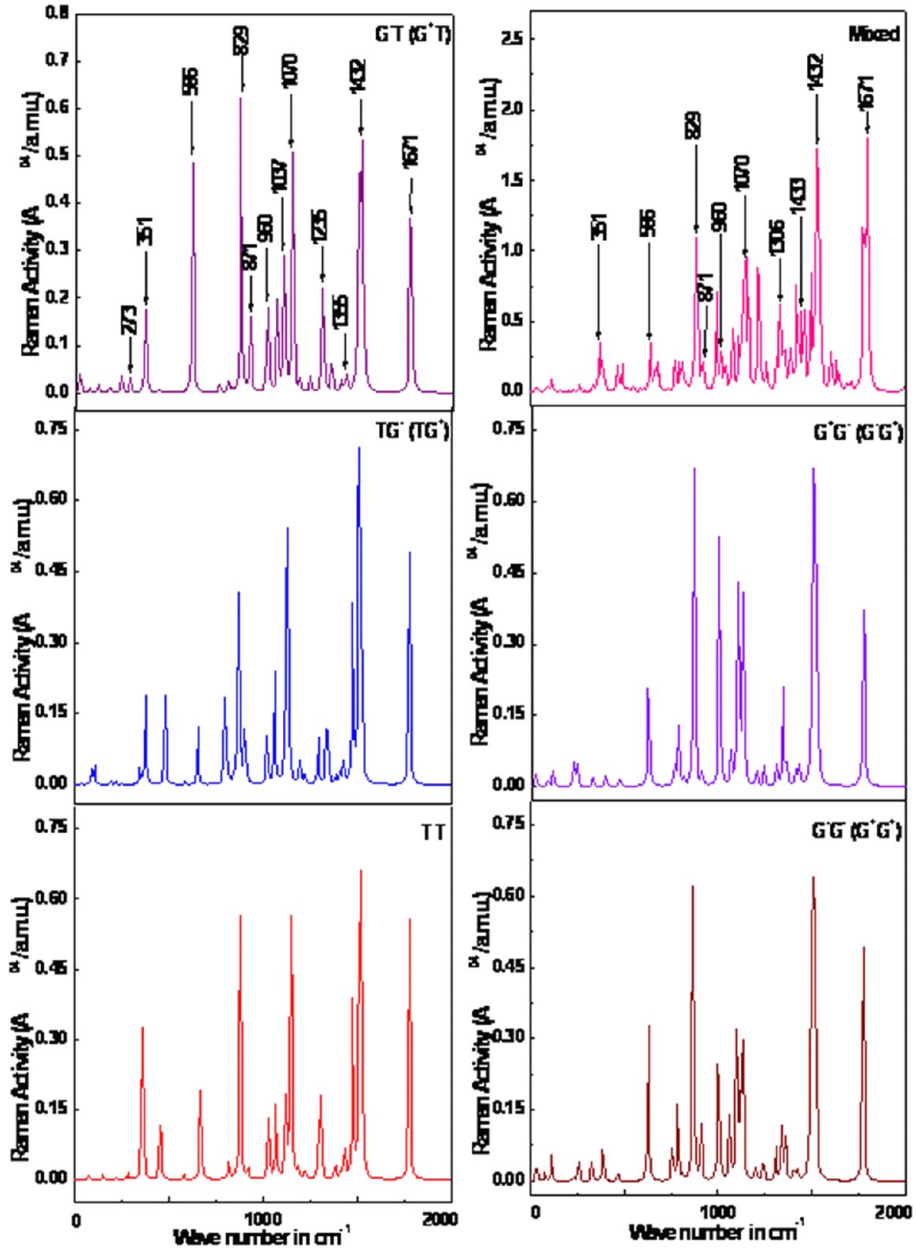

Figure 3. The theoretically simulated gas-phase Raman spectra of the TT, TG^- (enantiomeric form TG^+), G^-T (enantiomeric form G^+T), and G^-G^- (enantiomeric form G^+G^+), G^+G^- (enantiomeric form G^-G^+) and mixture of all the forms of the EP molecule in 0−2000 cm^{-1} region using the MP2/aug-cc-PVTZ level of theory.

The FTIR and the Raman spectrum (RS) of the EP molecule in neat liquid recorded at room temperature (ca. 25 °C) are shown in Figure 2(a−c), respectively. Figures 3 and 4 show the theoretically simulated Raman spectra of the TT, TG^-, G^-T, G^-G^-, and G^+G^- forms and the mixture of all five rotameric forms of the EP molecule. The primary aim of recording the RS and FTIR spectra is to apprehend the existence/existences of the preferential rotameric forms of the EP molecule from the assignment of their respective vibrational signatures. The definitions of internal and local symmetry coordinates are tabulated in Table TS2. Table1 lists the experimentally observed FTIR, RS band frequencies of the EP molecule. The theoretically computed vibrational frequencies of the different forms of the EP molecule are also shown in Table 1 along with their tentative assignments, as provided from the potential energy distributions (PEDs). The detailed vibrational analyses of various forms of the EP molecule are shown in Table TS3. The observed disagreement between the theory and the experiment could be a consequence of the anharmonicity and also may be due to the general tendency of the quantum chemical methods to overestimate the force constants at the exact equilibrium geometry.[12] Despite the fact, one can see that there is a general concordance regarding the Raman intensities as well as the position of the peaks between the experimental and the calculated spectra.[13]

The FTIR spectrum of the EP molecule in liquid state is characterized by a large number of vibrational signatures; many of them appear as doublets or multiplets. The RS of the EP molecule recorded in liquid state exhibit much less but well resolved vibrational signatures compared to that recorded in the FTIR. The modes arising principally from the torsion, stretching, bending, twisting, deformation, and rocking

dx.doi.org/10.1021/jp404247v | J. Phys. Chem. A 2013, 117, 4838−4850

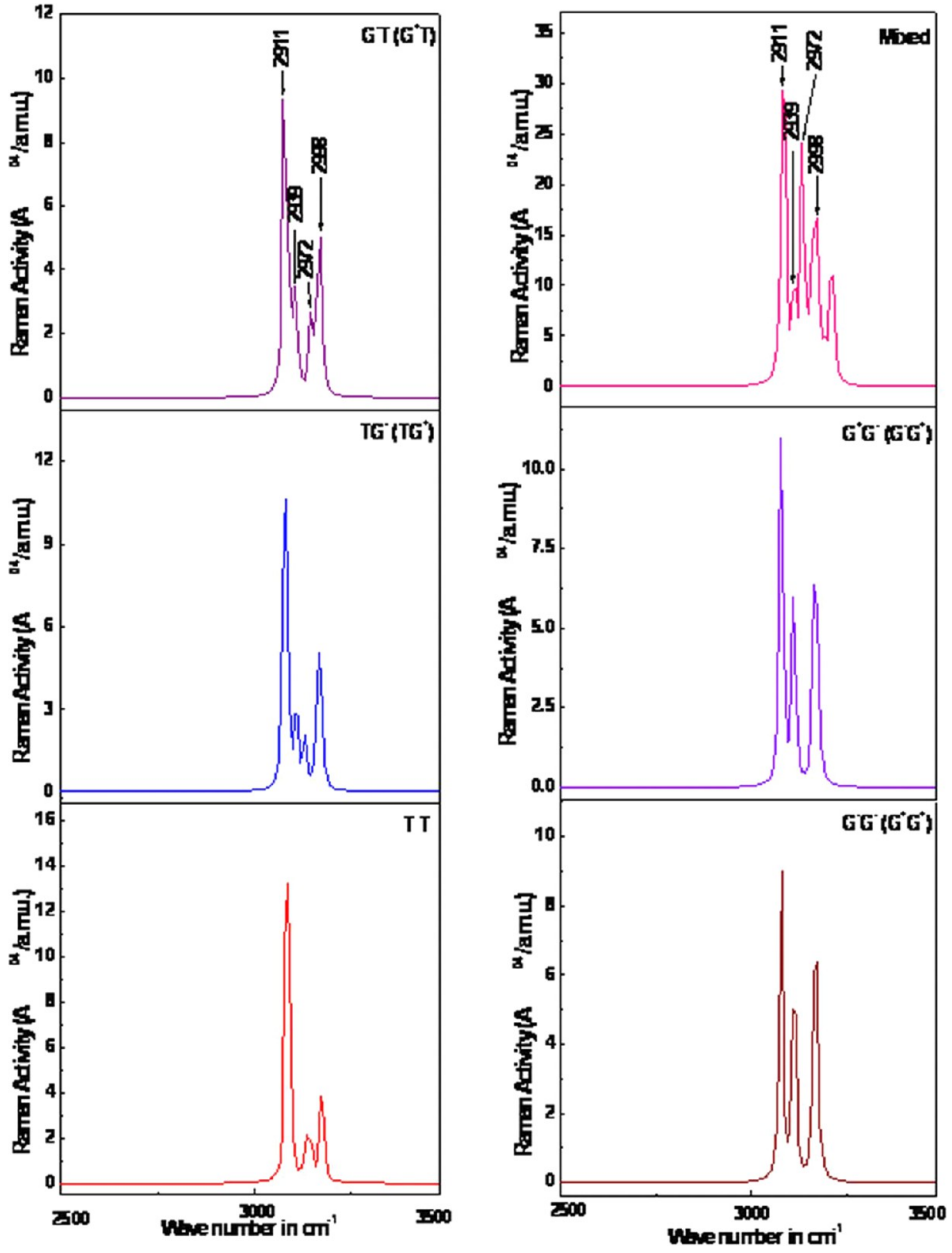

Figure 4. The theoretically simulated gas-phase Raman spectra of the TT, TG^- (enantiomeric form TG^+), G^-T (enantiomeric form G^+T), G^-G^- (enantiomeric form G^+G^+), and G^+G^- (enantiomeric form G^-G^+) and mixture of all the forms of the EP molecule in 2000−4000 cm^{-1} region using the MP2/aug-cc-PVTZ level of theory.

vibrations of the five different rotameric forms of the EP molecule are identified. In the assignment of the vibrational frequencies, the literature concerning this and related molecules has been considered.[14]

A significant conclusion can be drawn from the appearance of very strong and well resolved bands in the RS and FTIR spectra of the EP molecule at around 2944 and 866 cm^{-1}. The band at ∼2944 cm^{-1} (calcd. 2940 cm^{-1} for TG^-, 2939 cm^{-1} for G^-T, 2939/2941 cm^{-1} for G^-G^-, and 2939.2/2939.7 cm^{-1} for the G^+G^- form of the EP molecule) has considerable contribution from υ (C_6−H_{13}), υ (C_6−H_{14}) stretching vibrations originating from TG^-, G^-T, G^-G^-, and G^+G^- molecular forms of the EP molecule. The other band at ∼866 cm^{-1} (calcd. at 855/860/860 cm^{-1} for the $TG^-/G^-G^-/G^+G^-$ form of the molecule) has a prevailing contribution from υ (O_5−C_6) stretching vibration arising from the TG^- form of molecule and/or β (C_6−C_7−H_{15}) bending; υ (O_5−C_6) and υ (C_6−C_7) stretching vibrations arising from the G^-G^-; G^+G^- forms of the EP molecule. Thus, the appearance of the above-mentioned vibrational signatures mark the presence of the TG^-, G^-T, G^-G^-, G^+G^-, and G^-G^-; G^+G^- forms of the EP molecule in the liquid state. Very strong and intense bands recorded at ∼2944, 2889, and 1438 cm^{-1} in the FTIR spectrum of the molecule also signify the presence of the TG^-, G^-T, G^-G^-, and G^+G forms of the EP molecule in the liquid state.

Considerable attention can be drawn regarding the band at ∼2994 cm^{-1} (calcd. at 2998 cm^{-1} for TT, 2996 cm^{-1} for TG^-, 2995/2997 cm^{-1} for G^-T, 2995/2996 cm^{-1} for G^-G^-, and 2995/2996 cm^{-1} for the G^+G^- form of the EP molecule) which is very strong in the FTIR spectrum but appear as a weak shoulder in the RS. The vibrational signature of this band has a significant contribution from the υ (C_7−H_{15}); υ (C_7−H_{16}), and

dx.doi.org/10.1021/jp404247v | J. Phys. Chem. A 2013, 117, 4838−4850

Table 1. Observed and Calculated Raman, IR Bands of the EP Molecule for Various Conformers, and Their Tentative Assignments[a]

		TT (C_s) (symmetry element)		TG$^-$ (C_1)		G$^-$T (C_1)		G$^-$G$^-$ (C_1)		G$^+$G$^-$ (C_1)	
FTIR	NRS	calcd freq	assinment [PED%]	calcd freq	assinment [PED%]	calcd freq	assinment [PED%]	calcd freq	assinment [PED%]	calcd freq	assinment [PED%]
		35	τ C(1) C(2) [73] (A'')	36	τ C(1) C(2) [75]	22	τ C(1) C(2) [63]	29	τ C(1) C(2) [69]	21	τ C(1) C(2) [62]
		74	τ O(5) C(6) [75] (A'')	87	τ O(5) C(1) [60]	70	τ O(5) C(6) [88]	75	τ O(5) C(1) [62]	81	τ O(5) C(1) [59]
	110 vvw			104	τ O(5) C(6) [58]	110	τ O(5) C(1) [61]	105	τ O(5) C(6) [76]	107	τ O(5) C(6) [69]
		127	τ O(5) C(1) [73] (A'')								
		146	δ C(1) O(5) C(6) [34] (A')								
				184	τ C(6) C(7) [27]	173	δ C(1) O(5) C(6) [36]				
	198 vvw							198	τ C(6) C(7) [36]	199	τ C(6) C(7) [35]
	212 vvw	211	τ C(2) C(3) [84] (A'')	209	τ C(2) C(3) [88]			220	τ C(2) C(3) [48]	216	δ C(1) C(2) C(3) [24]
	234 vvw			236	τ C(6) C(7) [51]	230	τ C(2) C(3) [34]			229	δ C(1) C(2) C(3) [35]
						232	τ C(2) C(3) [32]				
	240 vw							243	δ C(1) C(2) C(3) [58]		
	256 vvw	255	τ C(6) C(7) [80] (A'')								
		271	δ C(1) O(5) C(6) [45] (A')			276	τ C(6) C(7) [38]				
	299 vw										
								312	δ C(1) O(5) C(6) [37]	310	δ C(1) O(5) C(6) [38]
	338 vw	343	δ O(5) C(6) C(7) [33] (A')	331	δ C(1) O(5) C(6) [39]						
				357	τ C(6) C(7) [38]	350	τ C(6) C(7) [37]				
	369 vs							366	δ O(5) C(6) C(7) [34]	376	δ O(5) C(6) C(7) [24]
406 vvw						415	β C(1) O(4) O(5) [45]				
		433	β C(1) O(4) O(5) [37] (A')					440	δ O(5) C(6) C(7) [29]	445	δ O(5) C(6) C(7) [35]
455 s	455 w			456	δ O(5) C(6) C(7) [31]						
	475 w										
		549	β_{op} C(1) O(4) O(5) [51] (A'')	554	β_{op} C(1) O(4) O(5) [46]						
584 s						586	r C(1) O(4) O(5) [39]			589	r C(1) O(4) O(5) [32]
598 s								595	r C(1) O(4) O(5) [29]		
	603 s			621	r C(1) O(4) O(5) [39]						
	645 vw	633	r C(1) O(4) O(5) [39] (A')								
668 w	665 vw										
	681 vw										
						718	β_{op} C(1) O(4) O(5) [58]	716	β_{op} C(1) O(4) O(5) [54]	720	β_{op} C(1) O(4) O(5) [58]
				754	r C(6) H_2 [40]			742	r C(6) H_2 [22]	740	r C(6) H_2 [25]
		768	r C(3) H_3 [24] (A'')	769	r C(3) H_3 [34]	760	r C(2) H_2 [41]	767	r C(2) H_2 [22]	766	r C(2) H_2 [24]
	790 w	775	r C(6) H_2 [30] (A'')			774	r C(6) H_2 [40]				
802 vvs	804 vw										
		832	r C(7) H_3 [21] (A')	823	ν C(1) O(5) [17]	827	r C(7) H_3 [20]	819	ν C(1) O(5) [17]	820	ν C(1) O(5) [16]
866 vvs	858 vs			855	ν O(5) C(6) [23]			860	r C(7) H_3 [19]	860	r C(7) H_3 [19]
		871	ν O(5) C(6) [23] (A')			874	ν O(5) C(6) [17]				
895 vs	889 w										
								949	ν C(2) C(3) [44]	949	ν C(2) C(3) [44]

dx.doi.org/10.1021/jp404247v | J. Phys. Chem. A 2013, 117, 4838−4850

Table 1. continued

		TT (C_s) (symmetry element)		TG$^-$ (C_1)		G$^-$T (C_1)		G$^-$G$^-$ (C_1)		G$^+$G$^-$ (C_1)	
FTIR	NRS	calcd freq	assinment [PED%]	calcd freq	assinment [PED%]	calcd freq	assinment [PED%]	calcd freq	assinment [PED%]	calcd freq	assinment [PED%]
		973	ν C(2) C(3) [28] (A′)	966	ν C(2) C(3) [34]	961	ν C(2) C(3) [43]				
992 sh	998 s			1005	ν O(5) C(6) [33]			1006	ν O(5) C(6) [22]	1007	ν O(5) C(6) [22]
1015 vvs		1011	ν O(5) C(6) [35] (A′)			1010	ν O(5) C(6) [21]				
1032 vs	1033 s					1039	r C(3) H_3 [42]	1037	r C(3) H_3 [41]	1039	r C(3) H_3 [42]
		1055	r C(3) H_3 [37] (A″)	1055	r C(3) H_3 [37]	1051	ν O(5) C(6) [25]	1052	ν O(5) C(6) [22]	1051	ν O(5) C(6) [22]
		1061	ν C(2) C(3) [37] (A′)	1061	ν C(2) C(3) [33]						
1069 vs				1070	r C(7) H_3 [39]			1068	r C(7) H_3 [44]	1069	r C(7) H_3 [44]
	1083 s	1087	r C(7) H_3 [36] (A′)			1086	r C(7) H_3 [37]				
	1097 s										
	1113 s										
1127 vvs		1123	r C(6) H_2[51](A″)	1132	r C(6) H_2 [34]	1123	r C(6) H_2 [51]	1135	r C(6) H_2 [45]	1135	r C(6) H_2 [45]
	1162 vw	1156	ν C(1) O(5) [45] (A′)	1154	ν C(1) O(5) [34]						
1171 vvs						1177	ν C(1) O(5) [27]	1174	ν C(1) O(5) [26]	1174	ν C(1) O(5) [26]
1190 vvs											
1222 vvs		1224	γ C(2) H_2 [76] (A″)	1224	γ C(2) H_2 [76]						
		1236	γ C(6) H_2 [86] (A″)			1235	γ C(6) H_2 [84]	1236	γ C(2) H_2 [48]	1237	γ C(2) H_2 [48]
1248 vs						1240	γ C(2) H_2 [45]				
	1262 s			1266	γ C(6) H_2 [87]			1266	γ C(6) H_2 [83]	1267	γ C(6) H_2 [83]
	1271 s										
1292 vs						1284	ω C(2) H_2 [40]	1285	ω C(2) H_2 [46]	1285	ω C(2) H_2 [45]
	1301 s	1307	ω C(2) H_2 [35] (A′)	1308	ω C(2) H_2 [38]						
1330 vs		1332	δ_s C(7) H_3 [42] (A′)	1331	δ_s C(7) H_3 [62]	1325	ω C(6) H_2 [40]	1326	δ_s C(7) H_3 [50]	1327	δ_s C(7) H_3 [53]
						1338	δ_s C(3) H_3 [79]	1336	δ_s C(3) H_3 [74]	1337	δ_s C(3) H_3 [76]
	1347 vw	1348	δ_s C(3) H_3 [84] (A′)	1347	δ_s C(3) H_3 [61]						
		1355	δ_s C(7) H_3 [38] (A′)	1350	ω C(6) H_2 [32]	1354	δ_s C(7) H_3 [44]	1347	ω C(6) H_2 [46]	1348	ω C(6) H_2 [48]
1377 vs											
	1392 sh	1395	β C(2) H_2 [98] (A′)	1394	β C(2) H_2 [94]						
						1416	β C(2) H_2 [88]	1415	β C(2) H_2 [87]	1416	β C(2) H_2 [87]
	1426 sh	1424	δ_{as} C(7) H_3 [98] (A″)	1422	δ_{as} C(7) H_3 [78]	1424	δ_{as} C(7) H_3 [90]	1422	δ_{as} C(7) H_3 [75]	1422	δ_{as} C(7) H_3 [75]
				1427	β C(6) H_2 [82]			1427	β C(6) H_2 [78]	1426	β C(6) H_2 [80]
		1431	δ_{as} C(3) H_3 [90] (A″)	1431	δ_{as} C(3) H_3 [90]						
1438 s		1434	δ_{as} C(7) H_3 [62] (A′)	1436	δ_{as} C(3) H_3 [82]	1434	δ_{as} C(7) H_3 [62]	1436	δ_{as} C(3) H_3 [89]	1436	δ_{as} C(3) H_3 [89]
		1437	δ_{as} C(3) H_3 [84] (A′)			1436	δ_{as} C(3) H_3 [89]				
				1441	δ_{as} C(7) H_3 [71]	1443	δ_{as} C(3) H_3 [80]	1440	δ_{as} C(7) H_3 [69]	1440	δ_{as} C(7) H_3 [70]
								1443	δ_{as} C(3) H_3 [76]	1443	δ_{as} C(3) H_3 [70]
	1454 vvs	1451	β C(6) H_2 [69] (A′)			1450	β C(6) H_2 [66]				
1484 (584 + 895)^b vs											
1656 sh		1679	ν C(1) O(4) [80] (A′)	1679	ν C(1) O(4) [79]	1678	ν C(1) O(4) [79]	1678	ν C(1) O(4) [78]	1677	ν C(1) O(4) [78]
1692 (802 + 895)^b vvs											
1737 (866 × 2)^c vvs	1734 vs										

dx.doi.org/10.1021/jp404247v | J. Phys. Chem. A 2013, 117, 4838−4850

Table 1. continued

		TT (C_s) (symmetry element)		TG$^-$ (C_1)		G$^-$T (C_1)		G$^-$G$^-$ (C_1)		G$^+$G$^-$ (C_1)	
FTIR	NRS	calcd freq	assinment [PED%]	calcd freq	assinment [PED%]	calcd freq	assinment [PED%]	calcd freq	assinment [PED%]	calcd freq	assinment [PED%]
2775 sh	2783 vw										
2889 vvs	2894 sh			2909	ν_s C(7) H_3 [98]	2907	ν_s C(3) H_3 [99]	2907	ν_s C(3) H_3 [99]	2908	ν_s C(3) H_3 [99]
								2908	ν_s C(7) H_3 [98]	2909	ν_s C(7) H_3 [98]
		2912	ν_s C(7) H_3 [99] (A′)			2911	ν_s C(7) H_3 [99]				
2919 vs	2916 sh	2915	ν_s C(3) H_3 [97] (A′)	2915	ν_s C(3) H_3 [97]						
		2919	ν_s C(2) H_2 [95] (A′)	2918	ν_s C(2) H_2 [96]						
		2924	ν_s C(6) H_2 [97] (A′)			2924	ν_s C(6) H_2 [98]				
2948 vvs	2944 vvs			2940	ν_s C(6) H_2 [97]	2939	ν_s C(2) H_2 [98]	2939	ν_s C(2) H_2 [95]	2939.2	ν_s C(2) H_2 [65]
								2941	ν_s C(6) H_2 [94]	2939.7	ν_s C(6) H_2 [64]
		2961	ν_{ans} C(2) H_2 [94] (A″)	2961	ν_{ans} C(2) H_2 [94]						
		2973	ν_{ans} C(6) H_2 [87] (A″)			2973	ν_{ans} C(2) H_2 [87]				
	2982 s					2987	ν_{as} C(3) H_3 [66]	2987	ν_{as} C(3) H_3 [70]	2987	ν_{as} C(3) H_3 [65]
				2991	ν_{as} C(7) H_3 [53]			2991	ν_{as} C(7) H_3 [55]	2991	ν_{as} C(7) H_3 [50]
2994 vvs		2998	ν_{as} C(7) H_3 [99] (A′)	2996	ν_{ans} C(6) H_2 [43]	2995	ν_{as} C(3) H_3 [98]	2995	ν_{as} C(3) H_3 [97]	2995	ν_{as} C(3) H_3 [98]
						2997	ν_{as} C(7) H_3 [99]	2996	ν_{ans} C(6) H_2 [40]	2996	ν_{ans} C(6) H_2 [44]
		3000	ν_{as} C(3) H_3 [99] (A′)	2999	ν_{as} C(3) H_3 [98]						
		3005	ν_{as} C(3) H_3 [95] (A″)	3004	ν_{as} C(3) H_3 [94]						
		3006	ν_{as} C(7) H_3 [88] (A″)			3006	ν_{as} C(7) H_3 [87]				
						3007	ν_{ans} C(2) H_2 [66]	3007	ν_{ans} C(2) H_2 [70]	3007	ν_{ans} C(2) H_2 [65]
				3014	ν_{as} C(7) H_3 [59]			3014	ν_{as} C(7) H_3 [54]	3014	ν_{as} C(7) H_3 [62]

[a]Key: vss, very very strong; vs, very strong; s, strong; w, weak; vw, very weak; vvw, very very weak; sh, shoulder; τ, torsion; δ, deformation; δ_{as}, asymmetric deformation; δ_{ans}, antisymmetric deformation; r, rocking; β, bending; β_{op}, out of plane bending; ν, stretching; ν_{as}, asymmetric stretching; ν_{ans}, antisymmetric stretching, ω, wagging. [b]Combination band. [c]Overtone band.

dx.doi.org/10.1021/jp404247v | J. Phys. Chem. A 2013, 117, 4838−4850

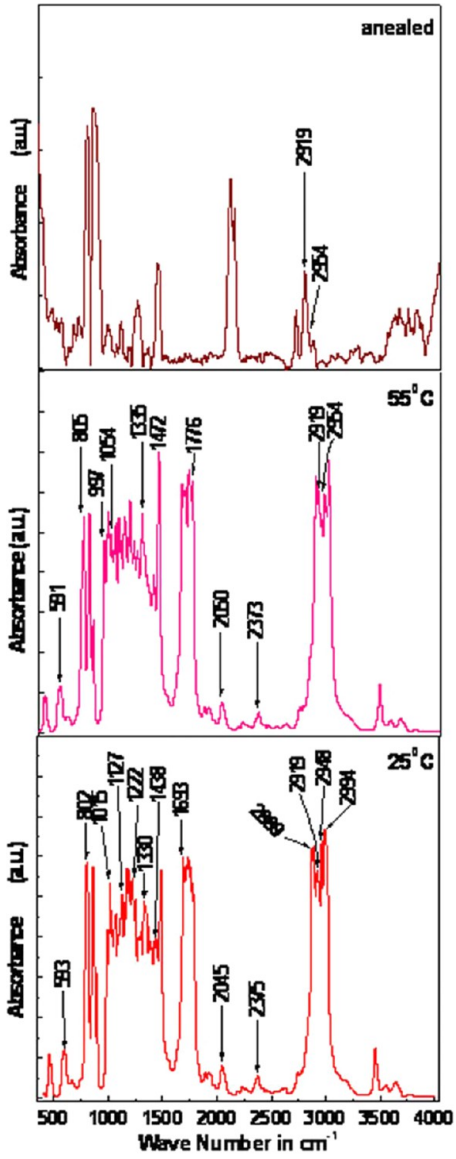

Figure 5. The FTIR spectra of the EP molecule in liquid state recorded at 25 °C and at 55 °C. The upper panel shows the FTIR spectrum of the annealed sample.

υ (C_7–H_{17}) stretching vibrations arising from TT; the G^-T form and/or υ (C_6–H_{13}); υ (C_7–H_{15}) stretching vibrations arising from the TG^-, G^-G^- ; G^+G^- forms of the EP molecule. The presence of the above-mentioned vibrational signature corroborates the presence of the TT; G^-T, TG^-, G^-G^-, and G^+G^- forms of the EP molecule in the liquid state. The presence of all five rotameric forms of the EP molecule is further supported by the appearance of strong vibrational signatures ∼1127, 1330, 1426, and 1438 cm^{-1} in the FTIR spectrum of the EP molecule.

Another band at ∼2919 cm^{-1} (calcd. at 2915/2919 cm^{-1} for TT and 2915/2918 cm^{-1} for the TG^- forms of the EP molecule), which appears as a very strong signal in the FTIR but weak in the RS spectrum of the molecule in liquid state, has been assigned to υ (CH_2) and υ (CH_3) symmetric stretching vibrations arising from the TT and TG^- forms of the molecule. The presence of the above-mentioned vibrational signature corroborates the presence of the TT and TG^- forms of the EP molecule in the liquid state.

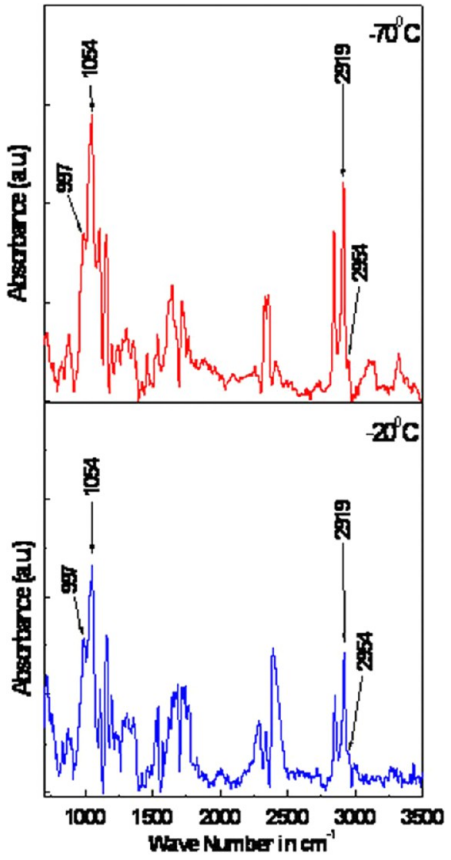

Figure 6. The FTIR spectra of the EP molecule in a liquid state recorded at −20 °C and at −70 °C.

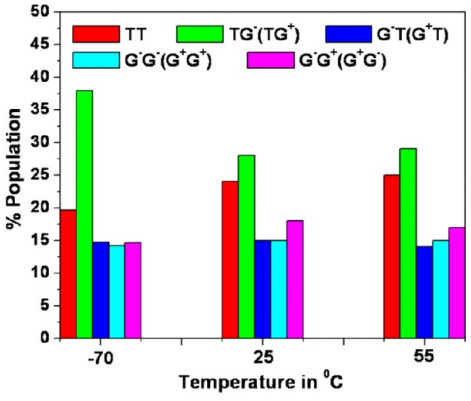

Figure 7. The bar diagram indicating the relative population of the TT, TG^- (enantiomeric form TG^+), G^-T (enantiomeric form G^+T), G^-G^- (enantiomeric form G^+G^+), and G^+G^- (enantiomeric form G^-G^+) forms of the EP molecule at 55 °C, 25 °C, and −70 °C.

The vibrational signature at ∼1454 cm^{-1} (calcd. at 1451/1450 cm^{-1} for the TT/G^-T form of the EP molecule), which appears as a strong signal in the RS but weak in the FTIR spectrum, has been ascribed to β (CH_2) bending vibrations stemming from the TT and/or the G^-T form of the EP molecule. A weak but prominent band at ∼787 cm^{-1} (calcd. at 775/774 cm^{-1} for the TT/G^-T form of the EP molecule) in the RS also marks the presence of either TT or G^-T or both forms of the EP molecule in the liquid state at room temperature. The vibrational signatures at ∼1015, 1156, 1222, 1394, and 1452 cm^{-1} which appear strong in the FTIR but

dx.doi.org/10.1021/jp404247v | J. Phys. Chem. A 2013, 117, 4838−4850

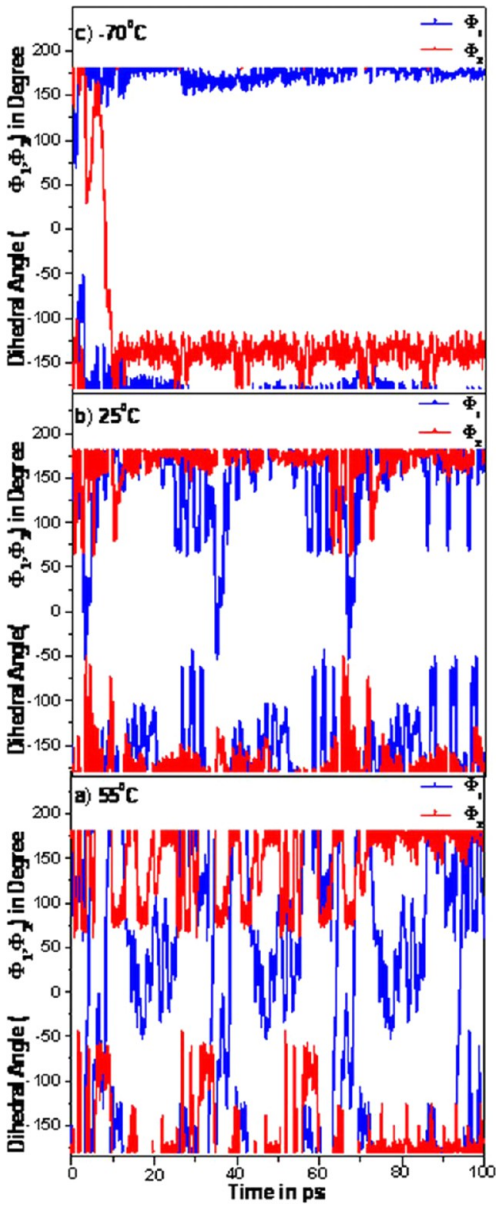

Figure 8. The variation of the superimposed dihedral angles φ_1 ($C_3-C_2-C_1-O_5$) and φ_2 ($C_1-O_5-C_6-C_7$) of the EP molecule with time as estimated from Car–Parrinello molecular dynamics studies simulated at a) 55 °C, b) 25 °C, and c) −70 °C.

weak in the RS spectrum of the molecule further corroborate the existences of the TT and/or G^-T forms of the EP molecule in the liquid state. Interestingly, the band at ∼1084 cm^{-1} which appears as a strong signal both in the RS and in the FTIR spectra also substantiates the existence of TT or G^-T or both forms of the EP molecule in the liquid state. Interestingly, the strong vibrational signatures at 1484, 1692, 1737 cm^{-1} are not estimated from the quantum chemical calculations. They may represent the combination and overtone bands. The 1484 cm^{-1} band may arise due to the combination of 584 + 895 = 1479 cm^{-1} bands, while the mode at 1692 cm^{-1} may emanate from the combination of 802 + 895 = 1697 cm^{-1} bands. The appearance of 1737 cm^{-1} band may be due to the overtone of 866 × 2 = 1732 cm^{-1} bands.

Thus, from the above vibrational analyses and from the relevant assignments of the vibrational signatures as shown in Table 1, the coexistences of all five rotameric trans forms (i.e., TT, TG^-, G^-T, G^-G^-, and G^+G^-) of the EP molecule have been envisaged in liquid state at room temperature.

This conjecture is further supported by the RS spectrum of the molecule recorded in 180–350 cm^{-1} wavenumber range. The RS spectrum, as shown in the inset of Figure 2b, is characterized by weak humps at ∼198 (calcd. at 198/199 cm^{-1} for the G^-G^-/G^-G^+ forms of the EP molecule), 212 (calcd. at 211/209/220/216 cm^{-1} for the $TT/TG^-/G^-G^-/G^-G^+$ forms of the EP molecule), 234 (calcd. at 236/230; 232/229 cm^{-1} for the $TG^-/G^-T/G^-G^+$ forms of the EP molecule), and at 256 cm^{-1} (calcd. at 255 cm^{-1} for the TT form of the EP molecule). All these bands have been ascribed to the torsional vibrations associated with the methyl group/groups of the TT, TG^-, G^-T, G^-G^-, and G^-G^+ forms of the EP molecule. The presence of these vibrational signatures in the RS spectrum of the neat liquid of the EP molecule marks the existences of all five rotameric forms (ca. TT, TG^-, G^- T, G^+G^-, and G^-G^+ forms) of the molecule at room temperature. The result is in accordance with that estimated from the vibrational analyses of the molecule (vide supra).

4.3. Temperature Dependent FTIR Spectra. In order to estimate the relative stability of different conformers of the molecule, the FTIR spectra of the EP molecule in liquid state have been recorded at different temperature domains one ranging from 25 to 55 °C and the other from −20 °C to −70 °C. They are shown in Figures 5 and 6, respectively. In the high temperature domain (Figure 5), the FTIR spectra of the molecule show slender but distinct variations in the relative intensity patterns particularly in the wavenumber range 800–1500 cm^{-1} and 2800–3000 cm^{-1}. These fluctuations in IR intensities may primarily be considered to be due to minor variation in the population of different conformers of the EP molecule with an increase in temperature, assuming Boltzmann distribution for the conformational mixture. Interestingly, the FTIR spectra of the molecule (particularly in the wavenumber range 2800–3000 cm^{-1}) recorded at low temperatures (Figure 6) are remarkably different from that recorded at room temperature (25 °C). The decrease in temperature is associated with the prominent increase in intensity of the 2918 cm^{-1} band. With the decrease in temperature, the band at 2919 cm^{-1} gains significant intensity with a concomitant decrease in intensity of 2889, 2954, and 2994 cm^{-1} bands. The 2919 cm^{-1} band has been assigned to υ (CH_2) and υ (CH_3) symmetric stretching vibrations arising from the TT and TG^- forms of the molecule (vide ante). The presence of the above-mentioned vibrational signature at ∼2919 cm^{-1} together with the decrease in intensity of the neighboring bands at ∼2889, 2954, and 2994 cm^{-1} corroborate the preponderance of the TT and TG^- forms of the EP molecule in the liquid state at low temperature. The preferential existences of the TT and TG^- forms of the EP molecule are further substantiated by the presence of distinct vibrational signature at ∼2919 cm^{-1} in the annealed FTIR spectrum (shown in Figure 5e) of the EP molecule recorded in the liquid state.

The relative populations of the different rotameric forms of the EP molecule at various temperature domains have been estimated from the ratio of the sum of the integrated intensities (i.e. I^{TT}, I^{TG^-}, I^{G^-T}, $I^{G^-G^-}$, $I^{G^+G^-}$) of the experimentally observed IR bands representing vibrational signatures of five rotameric forms of the EP molecule divided by the theoretically predicted

dx.doi.org/10.1021/jp404247v | J. Phys. Chem. A 2013, 117, 4838–4850

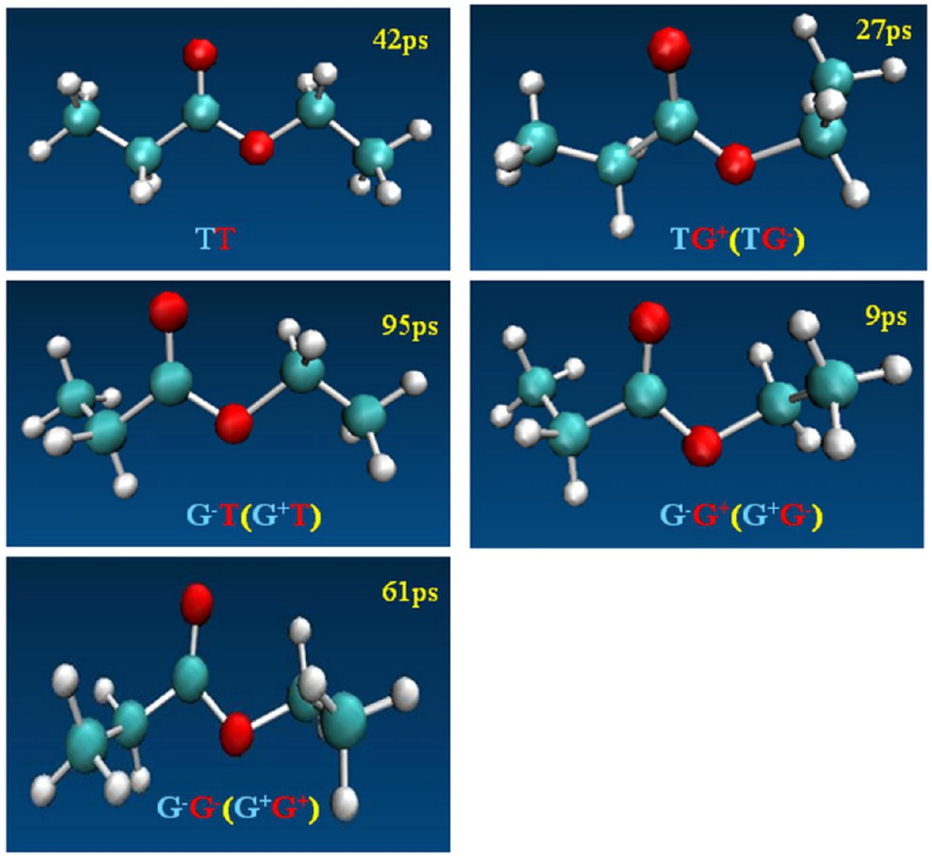

Figure 9. The snap shots of the molecular dynamics simulations captured at various ps time scales of the EP molecule at room temperature.

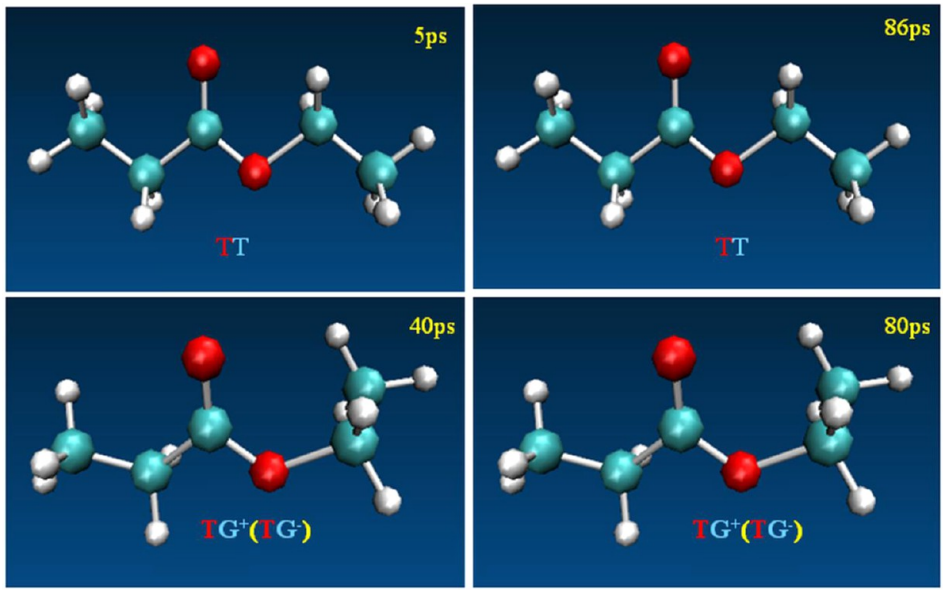

Figure 10. The snap shots of the molecular dynamics simulations captured at various ps time scales of the EP molecule at low temperature.

sums of absolute intensities (i.e. A^{TT}, A^{TG^-}, A^{G^-T}, $A^{G^-G^-}$, $A^{G^+G^-}$) of the respective bands taking two at a time.[15]

$$\frac{[Form_i]}{[Form_j]} = \frac{\sum_i I_i \sum_j A_j}{\sum_j I_j \sum_i A_i} \quad (2)$$

Figure 7 shows the bar diagram indicating the relative population of the five different forms of the molecule in the liquid state at room, high, and low temperature domains. The results indicate that at room temperature the population of the TT and TG^- forms of the EP molecule is ~24% and 28%, respectively, while the populations are ~15% for G^-T, 15% for G^-G^-, and 18% for the G^+G^- forms of the EP molecule. At low temperature (−70 °C), the population is dominated by the TG^- (~37%) and TT rotameric forms (~20%) of the EP molecule compared to the other G^-T, G^-G^-, G^+G^- forms

dx.doi.org/10.1021/jp404247v | J. Phys. Chem. A 2013, 117, 4838−4850

whose populations have been estimated to be ∼14%. At high temperature (55 °C) 25% of TT, 29% of TG^-, 14% of G^-T, 15% of G^-G^-, and 17% of G^+G^- forms of the EP molecule are estimated. The experimentally observed vibrational signatures of the molecule followed by the detailed vibrational analyses thus signify the preferential existences of the TT, TG^-, G^-T, G^-G^-, and G^+G^- forms of the EP molecule at room and also at high temperatures. The preponderant existences of the TT and TG^- forms of the molecule are estimated at low temperature. Among the TT and TG^- forms, the statistical preference toward the existence of the TG (TG^+/TG^-) form over the TT form of the EP molecule is also reflected from the vibrational analyses.

Interestingly, the calculated free energy (ΔG) values at room temperature (∼298.150 K) for the TT, TG^-, G^-T, G^-G^-, and G^-G^+ forms of the EP molecule as obtained from the MP2/aug-cc-pVTZ levels of theories are −217288.102, −217287.817, −217287.579, −217287.275, and −217287.278 kcal/mol, respectively. These results primarily indicate the existence of ∼29%, 26%, 16%, 14%, and 16% of the TT, TG^-, G^-T, G^-G^-, and G^-G^+ forms of the EP molecule at room temperature. The result is in harmony with that envisaged from the vibrational analyses of the molecule.

4.4. Car−Parrinello Molecular Dynamics Simulation Study. The conformational state of the EP molecule has been estimated from the Car−Parrinello molecular dynamics simulation study. The time evolutions of the dihedral angles φ_1 and φ_2, characterized by the $C_3-C_2-C_1-O_5$ and $C_1-O_5-C_6-C_7$ atoms, respectively, of the EP molecule have been estimated. When the dihedral angles φ_1, φ_2 are ±180°, the EP is said to be in the trans (T) form and when the angles are ±60°, the EP molecule is said to in the gauche/antigauche (G^+/G^-) form. The time evolution of the dihedral angles (φ_1, φ_2) of the EP molecule simulated at high (55 °C), room (25 °C), and low (−70 °C) temperatures are shown in Figure 8 (a−c). Figure 8 (a−c) shows the superimposed time series plots which depict the synchronized variations of both the dihedral angles φ_1 and φ_2 of the EP molecule at the above-mentioned temperatures. The variations of φ_1 and φ_2 with time over a 100 ps time scale for the EP molecule simulated at 55 and 25 °C [Figure 8 (a,b)] are characterized by distinct crests and pits characteristic of the T, G^+, and G^- forms of the EP molecule. The time series plots as shown in Figure 8 (a,b) thus mark the concomitant presence of the TT, TG^-, G^-T, G^-G^-, and G^+G^- forms of the EP molecule at room (25 °C) and at high (55 °C) temperatures. This result is in accordance with our conjecture as suggested from the vibrational analyses (vide ante). However, the variations of φ_1 and φ_2 with time for the EP molecule at low temperature (−70 °C) is markedly different from that estimated at room and high temperatures. The time evolutions of the dihedral angles φ_1 and φ_2 for the EP molecule simulated at low temperature (−70 °C) (Figure 8c) exhibit distinct crests diagnostic of the T form of the EP molecule, along with wells, designative of the G^- and G^+ forms of the EP molecule. The superimposed time series plots (Figure 8 c) showing the variation of the dihedral angles φ_1 and φ_2 simultaneously mark the presence of the TT and TG^- forms of the EP molecule at low temperature (−70 °C). This result is also in harmony with our conjecture as suggested from the vibrational analyses (vide ante). The snap shots of the molecular dynamics simulations captured at various ps time scales as shown in Figures 9 and 10 clearly indicate the possible existences of the TT and TG^- forms of the EP molecule at low temperature and the TT, TG^-, G^-T, G^-G^-, and G^+G^- forms of the EP molecule at room temperature. The Car−Parrinello molecular dynamics simulation studies are thus in accordance with the results as obtained from the detailed vibrational signatures of the EP molecule estimated at room, high, and low temperatures.

5. CONCLUSION

The conformational preferences of various rotameric forms of ethyl propionate (EP) molecules have been investigated from the Raman and FTIR spectra of the EP molecule aided by ab initio quantum chemical and Car−Parrinello molecular dynamics simulation studies. The optimized structural parameters of all the different rotameric forms of the EP molecule have been estimated from the MP2/aug-cc-pVTZ level of theory. The vibrational modes of the EP molecule have been assigned for the first time on the basis of potential energy distributions (PEDs). The analyses of the vibrational signatures of the EP molecule, as obtained from the Raman and temperature dependent FTIR spectra, envisage the coexistences of the TT, TG^- (TG^+), G^-T (G^+T), G^-G^- (G^+G^+), and G^+G^- (G^-G^+) forms of the EP molecule at room and at high temperatures, whereas at low temperature (ca. ∼−70 °C), the TT and TG^- forms of the EP molecule are estimated to be preponderant. These results are also in close harmony with that estimated from the Car−Parrinello molecular dynamics studies of the EP molecule simulated at high, room, and low temperatures. The ab initio molecular dynamics is observed to be a useful tool for the conformational analysis of the EP molecule.

■ ASSOCIATED CONTENT

Ⓢ Supporting Information

The selected optimized structural parameters, dipole moments, and rotational constants are shown in Table TS1,.The definition of internal and local symmetry coordinates of the EP molecule are shown in Table TS2. The observed and calculated Raman, IR bands of the EP molecule for various conformers in detail and their tentative assignments are shown in Table TS3. This material is available free of charge via the Internet at http://pubs.acs.org.

■ AUTHOR INFORMATION

Corresponding Author

*Phone: +91-33 - 24624554. Fax: +91-33-24626869. E-mail: joydeep72_c@rediffmail.com.

Notes

The authors declare no competing financial interest.

■ ACKNOWLEDGMENTS

The authors are deeply indebted to Professor Tarasankar Pal and Dr. Sougata Sarkar of Chemistry Department, IIT Kharagpur for recording the Raman spectrum. Joydeep Chowdhury would like to thank DAE-BRNS for the financial support through the Research Project (Project No. 2012/37P/27/BRNS/).

■ REFERENCES

(1) Bartley, J. P.; Schwede, A. M. Production of Volatile Componds in Ripening Kiwi Fruit (Actinidia Chinensis). *J. Agric. Food Chem.* **1989**, *37*, 1023−1025.

(2) Perez, A. G.; Rios, J. J.; Carlos, S.; Olias, J. M. Aroma Components and Free Amino Acids in Strawberry Variety Chandler During Ripening. *J. Agric. Food Chem.* **1992**, *40*, 2232−2235.

(3) Vibeke, F. A.; Kristian, B. Ø.; Solvejg, J.; Ole, J. N.; Matthew, S. J. Atmospheric Chemistry of Ethyl Propionate. *J. Phys. Chem. A* **2012**, *116*, 5164−5179.
(4) Frisch, M. J.; Trucks, G. W.; Schiegel, H. B.; Scuseria, G. E.; Robb, M. A.; Cheeseman, J. R.; Montgomery, J. A., Jr.; Vreven, T.; Kudin, K. N.; Burant, J. C.; et al. *Gaussian 03*; Gaussian, Inc.: Pittsburgh, PA, 2003.
(5) Mőller, C.; Plesset, M. S. Note on an Approximation Treatment for Many-Electron Systems. *Phys. Rev.* **1934**, *46*, 618−622.
(6) (a) Wilson, E. B.; Decius, J. C.; Cross, P. C. *Molecular Vibrations: The Theory of Infrared and Raman Vibrational Spectra*; McGrawHill: New York, 1955. (b) Kuwae, A.; Machida, M. The CH Out-of-Plane Deformation Vibrations of Monosubstituted Benzenes and Effect of Substituents on Related Force Constants. *Spectrochim. Acta, Part A* **1978**, *34*, 785−791.
(7) CPMD. Copyright IBM Corp 1990−2008, Copyright MPI fur Festkorperforschung Stuttgart 1997−2001. http://www.cpmd.org/ (accessed May 18, 2013).
(8) (a) Nose, S. A Unified Formulation of The Constant Temperature Molecular Dynamics Methods. *J. Chem. Phys.* **1984**, *81*, 511−519. (b) Hoover, G. Canonical dynamics: Equilibrium Phase-Space Distributions. *Phys. Rev. A* **1985**, *31*, 1695−1697.
(9) Perdew, J. P.; Burke, S.; Ernzerhof, M. Generalized Gradient Approximation Made Simple. *Phys. Rev. Lett.* **1996**, *77*, 3865−3868.
(10) Troullier, N.; Martins, J. L. Efficient Pseudopotentials for Plane-Wave Calculations. *Phys. Rev. B* **1991**, *43*, 1993−2006.
(11) Humphrey, W.; Dalke, A.; Schulten, K. VMD: Visual Molecular Dynamics. *J. Mol. Graphics* **1996**, *14*, 33−38.
(12) (a) Chowdhury, J.; Sarkar, J.; Tanaka, T.; Talapatra, G. B. Concentration-Dependent Orientational Changes of 2-Amino-2-thiazoline Molecule Adsorbed on Silver Nanocolloidal Surface Investigated by SERS and DFT. *J. Phys. Chem. C* **2008**, *112*, 227−239. (b) Sarkar, J.; Chowdhury, J.; Talapatra, G. B. Adsorption of 4-Methyl-4*H*-1,2,4-triazole-3-thiol Molecules on Silver Nanocolloids: FT-IR, Raman, and Surface-Enhanced Raman Scattering Study Aided by Density Functional Theory. *J. Phys. Chem. C* **2007**, *111*, 10049−10061. (c) Panda, S.; Chowdhury, J.; Pal, T. Understanding the Enhancement Mechanisms in the Surface-Enhanced Raman Spectra of the 1,10-Phenanthroline Molecule Adsorbed on a Au@Ag Bimetallic Nanocolloid. *J. Phys. Chem. C* **2011**, *115*, 10497−10509. (d) Chandra, S.; Chowdhury, J.; Ghosh, M.; Talapatra, G. B. Adsorption of 3-Thiophene Carboxylic Acid on Silver Nanocolloids: FTIR, Raman, and SERS Study Aided by Density Functional Theory. *J. Phys. Chem. C* **2011**, *115*, 14309−14324.
(13) (a) Aroca, R. F.; Clavijo, R. E.; Halls, M. D.; Schlegel, H. B. Surface-Enhanced Raman Spectra of Phthalimide. Interpretation of the SERS Spectra of the Surface Complex Formed on Silver Islands and Colloids. *J. Phys. Chem. A* **2000**, *104*, 9500−9505. (b) Bolboaca, M.; Iliescu, T.; Paizs, Cs.; Irimie, F. D.; Kiefer, W. Raman, Infrared, and Surface-Enhanced Raman Spectroscopy in Combination with ab Initio and Density Functional Theory Calculations on 10-Isopropyl-10*H*-phenothiazine-5-oxide. *J. Phys. Chem. A* **2003**, *107*, 1811−1818.
(14) (a) Moravie, R. M.; Corset, J. Conformational Behaviour and Vibrational Spectra of Methyl Propionate. *Chem. Phys. Lett.* **1974**, *26*, 210−214. (b) George, W. O.; Hassid, D. V.; Maddams, W. F. Conformations of Some saturated Carbonyl compounds. Part II. Infrared Spectra of Ethyl Formate, Acetate, Propionate, and n-Butyrate, and, Ethyl n-Butryrate. *J. Chem. Soc., Perkin Trans 2* **1942**, 1798−1801.
(15) (a) Chandra, S.; Chowdhury, J.; Ghosh, M.; Talapatra, G. B. Genesis of Enhanced Raman Bands in SERS Spectra of 2-Mercaptoimidazole: FTIR, Raman, DFT, and SERS. *J. Phys. Chem. A* **2012**, *116*, 10934−10947. (b) Lipinski, L.; Nowak, M. J.; Kwiatkowski, J. S.; Leszczynski, J. Phototautomeric Reaction, Tautomerism, and Infrared Spectra of 6-Thiopurine. Experimental Matrix Isolation and Quantum-Mechanical (Conventional Ab Initio and Density-Functional Theory) Studies. *J. Phys. Chem. A* **1999**, *103*, 280−288.